

Structural changes in precipitated silica induced by external forces

Gerald Johannes Schneider and Dietmar Göritz

Citation: *J. Chem. Phys.* **132**, 154903 (2010); doi: 10.1063/1.3389480

View online: <http://dx.doi.org/10.1063/1.3389480>

View Table of Contents: <http://jcp.aip.org/resource/1/JCPSA6/v132/i15>

Published by the American Institute of Physics.

Additional information on J. Chem. Phys.

Journal Homepage: <http://jcp.aip.org/>

Journal Information: http://jcp.aip.org/about/about_the_journal

Top downloads: http://jcp.aip.org/features/most_downloaded

Information for Authors: <http://jcp.aip.org/authors>

ADVERTISEMENT

physicstoday

Comment on any
Physics Today article.

Physics Today / Volume 65 / July 2012
Previous Article | Next Article
Measured energy in Japan
David von Seggern
(vonseg@seismo.unr.edu) University of Nevada
July 2012, page 10
DIGITAL OBJECT IDENTIFIER
<http://dx.doi.org/10.1063/PT.3.1619>
The article by Thorne Lay and Hiroo Kanamori is an interesting one. It discusses the energy released by the 2011 earthquake in Japan. The authors estimate that the earthquake released approximately five times as much energy as the atomic bombing of Nagasaki. This is a significant finding. However, the authors do not provide any references for their calculations. This is a major flaw in their argument. By the act of hitting a ball with a bat, one calculates the force energy to deliver the ball to its new location, but one must also take into account that the ball extended its energy release to that which became struck by the ball as its momentum ceased and passed energy to the struck team. Therefore the parameters of the damage extend into the future when the received energy to that pushed upon later becomes released in a new event. Perhaps calculations of one added that in while another's calculations did not. E.M.C.
Written by Edgar McCarville, 14 July 2012 19:59

Structural changes in precipitated silica induced by external forces

Gerald Johannes Schneider^{1,a)} and Dietmar Göritz²¹*Institut für Festkörperforschung, Neutronscattering and JCNS, Forschungszentrum Jülich, 52425 Jülich, Germany*²*Institut für Physik, Universität Regensburg, 93040 Regensburg, Germany*

(Received 1 August 2009; accepted 23 March 2010; published online 21 April 2010)

The morphology of pure precipitated silica, silica filled in polydimethylsiloxane rubber, and silica filled in styrene butadiene rubber was studied by means of small-angle X-ray scattering experiments. The silica at a length scale of a few nanometers consists of primary particles, which form aggregates, and clusters with aggregates as basic units. It is evidenced that the aggregate branching, represented by the mass fractal dimension, and the aggregate diameter are different if pure silica and silica in rubber are compared. Contrary, the size of the primary particles and their surface are not influenced. It is demonstrated that the change in the aggregate morphology is due to the external mechanical forces appearing during the mixing process. This is achieved by model experiments using a pistil and a mortar and a composite with different silica fractions. By that means, a systematic change in the morphology with grinding time is observed. Then, the experiments on the composite demonstrate that the major contributions to the mass fractal dimensions are due to the external mechanical forces. In order to test reproducibility and universal validity in the case of precipitated silicas, independent experiments on one silica and further silicas are performed. Several important conclusions are obtained from the study. First, it is shown that a comparison of different pure silica samples without knowing their history may be difficult or questionable. Second, it becomes evident that it is not sufficient to provide only a description of the materials, rather than the details of the sample treatment have to be reported. Therefore, solely the characterization of the morphology of the pure silica is not sufficient to be compared to the mechanical properties of the composites. © 2010 American Institute of Physics. [doi:10.1063/1.3389480]

I. INTRODUCTION

Soft matter composites, e.g., mixtures of hard particles and soft polymers, are a very important class of materials offering a variety of different properties which are exploited by many applications. For example, the modulus of natural rubber filled with silica or carbon black can be significantly enhanced. This change in the mechanical properties can be attributed to the increase in the viscosity if particles are added to a fluid as predicted by Einstein.^{1,2} In the case of rubber, additionally, interactions of the polymer chains with the filler, which depend on its surface or branching, affect the complex modulus of composites.³⁻⁷

In order to study the morphology of the filler particles, microscopic experiments seem to be very appropriate, e.g., transmission electron microscopes provide structural information possessing a resolution at the nanometer length scale. Consequently, such an experiment was exploited to study, e.g., the morphology of carbon black more than 60 years ago.⁸ As reported by the very recent review of Luginsland⁹ even nowadays the pure particles, or the fillers washed out of the polymer matrix, are studied by microscopic experiments. Then the structure of silica or carbon black is related to the macroscopic properties of the composites.

Recently, it was shown that uniaxial external forces can

align the filler particles at the length scale of a few nanometers and by that means change their structure.¹⁰⁻¹³ If the particles and the rubbery matrix are mixed, mechanical forces will occur due to the mixer, and due to particle-particle and particle-polymer interactions, and therefore the structure is possibly changed.⁷ Therefore, the cluster size of the pure silica and the silica dispersed within a rubbery matrix possibly differs.^{14,15} In particular, in the case of both precipitated and pyrogenic silica dispersed in a solvent, the break up of clusters with diameters in the range of 500 nm or larger due to ultrasonic irradiation was demonstrated.^{16,17} An influence of the ultrasonic irradiation experiments on the structure at a length scale of 100 nm and below was not observed, possibly because this was not the topic of the cited study. However, structural changes in silica below 100 nm seem to be possible, in particular, structural changes such as the cracking of clusters and rupture of weak arms, and by that means compacting the clusters.

At present, a full study which addresses possible changes in the morphology due to the mixing process at the length scale of about (10–100) nm does not exist, neither for precipitated nor for pyrogenic silica. In order to reveal such influences, the present work focuses on several precipitated pure silicas before and after the influence of an external force, and precipitated silica dispersed into different polymer composites, studied by means of small-angle x-ray scattering (SAXS) experiments. First, it is shown that the morphology

^{a)}Electronic mail: g.j.schneider@fz-juelich.de.

of pure silica and silica in the polymer differs. Second, evidences are presented that these differences can be attributed to external forces due to the mixer acting during the mixing process. Finally, it is demonstrated that filler-filler interactions play a less important role if compared to the forces induced by the external mixer. Therefore, for the first time, it is shown that it is not sufficient to compare the structure of pure silica or the silica washed out of the matrix, to, e.g., the results obtained from mechanical experiments on the composite material.

II. EXPERIMENTAL SECTION

A. Samples

Several precipitated silicas, possessing the trade names VN2, VN3, and U7000, kindly provided by Evonik Degussa GmbH, Köln, Germany, were studied by means of SAXS experiments. Detailed descriptions of these precipitated silicas and their synthesis are available in several review articles.^{9,14,15} The polydimethylsiloxane (PDMS) (SiO(CH₃)₂)_n rubber filled with precipitated silica VN3 was kindly provided by Lanxess (Leverkusen, Germany). The volume fraction of the filler varies from 9 to 23 vol %. To cure the rubbers the manufacturer used 0.4 phr Varox 50 and heated the mixtures 10 min at 175 °C using a press. Then, the samples were vulcanized for 10 min at 170 °C and annealed for 6 h at 200 °C. The styrene butadiene rubber (SBR) filled with silica was kindly provided by the Deutsches Institut für Kautschuktechnologie e.V., Hannover, Germany. The mixing process of SBR (SBR 1500, Lanxess, Leverkusen, Germany) and precipitated silica VN3 (Evonik Degussa GmbH, Köln, Germany) consisted of two major steps. First, the silica was added together with the stearic acid (2 phr) to the rubber and then mixed for 4 min using an internal mixer at 40 °C and a rotor speed of 50 rpm. Second, the vulcanization system was incorporated into the master batches on a two-roll-mill at 60 °C and a rotor speed of 16 rpm (first roll) and 20 rpm (second roll). The silica fraction was 9 vol %. Additionally the samples contain 1.5 phr sulfur and 0.5 phr vulcavit.

B. SAXS experiments

The SAXS experiments were performed at the beamline BW4 of the DORIS III storage ring at the Hamburger Synchrotronstrahlungslabor (HASYLAB) at the Deutsches Elektronen-Synchrotron (DESY), Hamburg (Germany). The measurements using the standard transmission configuration^{18,19} and were carried out at a fixed energy of 8979 eV, corresponding to a wavelength $\lambda=0.138$ nm. The scattered intensity was recorded by the two two-dimensional detectors (Gabriel type and Mar CCD). The intensity curves $I(q)$ were obtained by radially averaging and appropriate subtraction of the background. To enlarge the accessible range of momentum transfer q [$q=(4\pi/\lambda)\sin\theta$, where 2θ is the scattering angle] and thus the accessible length scale, different sample-detector distances (2 and 12 m) were

combined. Due to a recent upgrade, i.e., a better collimation of the incoming radiation, lower q -values are accessible and therefore several diagrams exhibit a larger q range.²⁰

III. THEORY

The silicas studied by the present work consist of primary particles which form aggregates due to the high volume concentrations of the samples involved. The aggregates are the basic units for larger clusters. By that means, a hierarchical structure, consisting of several characteristic length scales, is created. Such an object can be reasonably well described by the concept of fractals. Therefore, most conveniently, the scattering diagrams of silica can be analyzed²¹ and the measured intensity I can be decomposed in the scattering of the primary particles, the aggregates, and larger clusters. In a reasonable approach, the primary particles can be represented by spheres with a rough surface, represented by the so-called surface fractal dimension d_s .²² For example, if the surface is smooth $d_s=2.0$ and if $d_s=3.0$, the surface is infinitely rough.²¹ The scattered intensity of a fractal surface is simply²¹

$$I \propto q^{-(6-d_s)}. \quad (1)$$

Similarly, the aggregates which consist of the primary particles can be described by means of a mass fractal dimension d_f , which represents the branching. For example, if the object is linear then $d_f=1$. When a homogeneous sphere is considered, then $d_f=3$. Similarly to Eq. (1) (Ref. 21),

$$I \propto q^{-d_f}. \quad (2)$$

Therefore, by means of a double logarithmic plot of the intensity, the slope provides a simple access to the surface roughness or to the mass fractal dimension. Fortunately the slopes usually observed are different and therefore the mass and surface fractal ranges can be distinguished very easily.

Frequently, the particles involved are polydisperse. Therefore, characteristic oscillations, representing the diameter, which would be observed in the scattering diagrams of spheres if only a single diameter is present, are smeared out. In such a case, the positions of the crossovers q_c between the fractal ranges provide the diameter of the primary particles d by $d=2\pi/q_c$.²³ However, in general, it is very difficult to determine accurate values because usually the crossover is very broad. Therefore, if the diameter of particles should be determined, it is convenient to fit the scattered intensity by means of a simple model for the primary particles and the aggregates. This is achieved by decomposing the scattered intensity in a particle and a structure factor,²⁴ i.e.,

$$I \propto S \cdot P. \quad (3)$$

The particle factor P of a polydisperse sphere can be most conveniently modeled by the Beaucage model^{22,25-29}

$$P = G \exp\left(-\frac{q^2 R_g^2}{3}\right) + B \cdot (q^*)^{-(6-d_s)} \quad (4)$$

with

$$q^* = \frac{q}{(\operatorname{erf}(qR_g/\sqrt{6}))^3}.$$

R_g denotes the radius of gyration of the spherical particles, which is connected to the radius R by $R_g^2 = 3/5R^2$. In the case of monodisperse spheres with smooth surfaces, the prefactor B is the Porod constant and G is the Guinier prefactor.²² The meaning of the prefactors if the particles are polydisperse and possess a rough surface are exhaustively described by Beaucage.^{22,25–29} Moreover, the structure factor S for fractals derived by Teixeira is used^{30,31}

$$S(q, \xi, r_0, d_f) = 1 + \frac{\Gamma(d_f + 1)}{(qr_0)^{d_f}} \left(1 + \frac{1}{(q\xi)^2} \right)^{1-d_f/2} \times \frac{\sin[(d_f - 1)\arctan(q\xi)]}{(d_f - 1)}. \quad (5)$$

The radius of gyration of the clusters is represented by ξ . If the aggregates form larger clusters, then the aggregates can be considered as basic units of these clusters. This is simply included in Eq. (3) by the multiplication of a second structure factor and replacing the R_g of the particles by ξ and introducing a mass fractal dimension d_{m2} . In general, the clusters have a mass fractal dimension lower than 3 and therefore the generalized equation

$$\xi^2 = 2d_f(d_f + 1)/((d_f + 2)(d_f + 5))R^2 \quad (6)$$

has to be used instead the simple relation between the radius of gyration and perimeter of the cluster.³²

In the present work, first, the fractal dimensions were determined applying Eqs. (1) and (2). Using the values determined by that means, the diameters are obtained without risking artificial contributions due to a large amount of independent parameters by applying the described model function independently.

As indicated, usually the samples are polydisperse; therefore, instead of Eq. (3), more sophisticated approaches are required.^{33–35} Fortunately, in the case of the silica studied in the present work the width of the diameter distributions are usually very narrow³⁶ and therefore shift the crossover only slightly,²³ but do not introduce new features in the scattering diagram, except the smearing of the oscillations. Furthermore, although some diameter distributions are accessible in the literature, by far, not all of the samples studied in the present work are tabulated. In particular, no general theoretically derived solution exists which allows to include size distributions in the particular case of hierarchical structures. Finally, in order to reveal changes due to external forces, only relative values are of interest and therefore the experimental justification is presented below. In particular, due to the mentioned reasons, effects due to polydispersity are neglected in the present work to avoid artificial contributions, which are only related to the analysis technique but not to the scattering diagrams.

IV. RESULTS AND DISCUSSION

Figure 1 shows the scattering diagrams of the three pure precipitated silicas VN3 and the silica VN3 in two different composites. Some diagrams exhibit a larger q -window due to

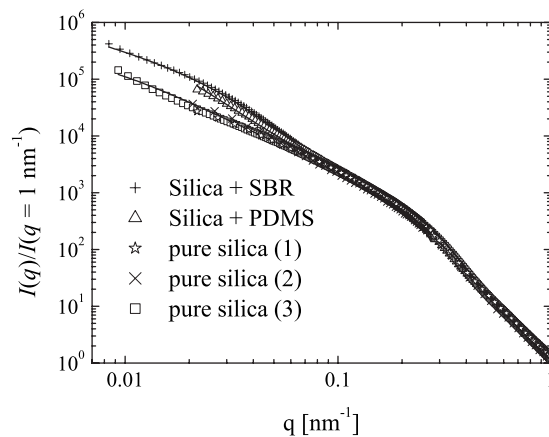


FIG. 1. Scattered intensity as a function of q of pure silicas VN3 and of the silica-rubber composites (filler fractions: 9 vol %). The lines represent fits with the model function.

the recent upgrade of the small-angle scattering instrument as described in the literature.²⁰ Silica VN3 (1) and silica VN3 (2) represent the scattering diagrams of two different samples taken from the same VN3 stock. Silica VN3 (3) is taken from a different container. Furthermore, the scattering diagrams of silica VN3 in two different composites, silica VN3 in SBR and silica VN3 in PDMS rubber, are depicted. The lines represent fits with the model function as explained in Sec. III. If the diagrams of pure silica and silica in the composites are compared, pronounced differences below $q \approx 0.08 \text{ nm}^{-1}$ are observed. Contrary, no differences are visible for larger q -values. Moreover, within the full range, the scattering diagrams of silica VN3 (1), silica VN3 (2), and silica VN3 (3) are almost identical. All of the curves exhibit the same crossover at $q_c \approx 0.2\text{--}0.3 \text{ nm}^{-1}$ and the scattering diagram of silica in the SBR matrix shows a pronounced, second crossover at $q \approx 0.04 \text{ nm}^{-1}$, representing the aggregate size. Additionally, in the case of the scattering curve of the pure silica (3) slight deviations of the fit and the experimental data at the very low q -values indicate a second crossover. Because of similar samples studied by a combination of several different scattering techniques and thus resolving significantly lower q -values in comparison to the present work, such a crossover is expected at the very low q -values of Fig. 1, e.g., Refs. 16 and 29. However, since the q -range accessible in Fig. 1 is limited, it is possible that the bending is due to damped oscillations from the aggregate itself, which is then a similar effect as the shoulder at the high q -side of the crossover due to the primary particles. Furthermore deviations from the power-law decay, i.e., the linear decay in the double logarithmic plot, are possibly generated by the fractal structure itself.³⁷ Therefore, future studies will have to access this range and to characterize this crossover in detail. In particular, it shows the need of accessing very low q -values in order to investigate the structure of silica or samples possessing hierarchical structures, similar to the experiments shown in the literature, e.g., Refs. 16 and 29. Due to the multilevel structure of silica, such a crossover exists^{16,29} for all of the samples studied here. Obviously, in the case of the other samples, the crossovers are completely outside of the observation window.

TABLE I. Radius of gyration R_g , radius of primary particles r , surface fractal dimension d_s , and mass fractal dimension d_f of the silicas.

Sample	R_g [nm]	R [nm]	d_s	d_f
VN3 (1)	8.7	11.3	2.00	1.74
VN3 (2)	8.7	11.3	2.00	1.87
VN3 (3)	8.7	11.3	2.00	1.68
VN2	10.5	13.6	2.00	1.83
U7000	9.6	12.5	2.00	1.92
VN3 in PDMS	8.7	11.3	2.00	2.16
VN3 in SBR	8.7	11.3	2.00	2.41

The radius of gyration, the surface fractal, and the mass fractal dimension are summarized in Table I. Furthermore, the primary particles are assumed to be spherically symmetric, and therefore the radius can be derived from the radius of gyration by $R^2=5/3R_g^2$. Because later the silicas VN2 and U7000 are studied, for the sake of completeness the calculated radii and values are tabulated. The q -ranges used for fitting the Eqs. (1) and (2) were $0.4\text{--}1\text{ nm}^{-1}$ for d_s and $0.02\text{--}0.2\text{ nm}^{-1}$ for d_f , respectively. The fitting error is very small, about 0.01 for the fractal dimensions and about 0.5 nm for the primary particle size. Actually, the chosen intervals are a compromise between the largest possible range and the perturbations due to the influence of the crossovers. Furthermore, scattering diagrams of fractals usually show deviations from the simple exponential decay, or the linear decay in the log-log representation.³⁷ Therefore, different q -ranges used for the local fit result in different fractal dimensions, with differences greater than the fitting error given above. However, if the q -range remains constant for all of the fits, only the absolute values are affected, but not the conclusions drawn out of the relative values. As shown by Table I, the experiments provide values which are very well reproducible. This is revealed in particular if the radius and the surface fractal dimension of the primary particles of VN3 are considered. The primary particles consist of chemically bonded SiO_2 molecules,^{9,14,15} and hence there are no reasons why differences should be observed. In particular, any mechanical force applied by the present work is not able to crack molecular bonds, and therefore neither the surface fractal dimension nor the diameter of the primary particle is expected to be changed. In contrast to Fig. 1, by comparing silica powder and silica in the composite, changes in the slope in the high q -limit have been reported in the literature.^{38–40} Marr *et al.*³⁸ attributed this effect to the formation of voids. Later, Rieker *et al.*³⁹ and Ehrburger-Dolle *et al.*⁴⁰ have discovered the influence of crystallization of the polymer on the slope and therefore an apparent growth of the slope with increasing the filler fraction. There is no indication of crystallization in the SBR matrix. In particular, there is no effect on the intensity in the high q -limit, i.e., on the surface fractal dimension. Therefore, the scattering curve of the pure SBR does not contain any indication of crystallization and the polymer scattering contribution is significantly lesser than that of the silica. Thus it is concluded that the intensity values at lower q 's are only determined by the silica scattering, and therefore the changes in the scattering dia-

grams are due to a different silica structure. A further indication that the values extracted reflect the silica is the radii of the primary particles. On the one hand, the radii are not changed if the pure silica and the silica polymer composites are compared. On the other hand, the absolute values are very close to those obtained with other scattering experiments and microscopic techniques.^{9,12,36,41,42} Very slight differences of scattering and microscopic experiments arise usually due to polydispersity²³ and are not considered further, in particular because the important result that the diameter of the primary particles is not influenced by the environment of the silica is not affected and even directly visible by a comparison of the scattering diagrams in Fig. 1. Furthermore, Table I shows that the mass fractal dimensions of the three VN3's vary more than expected from the experimental error. This demonstrates that fluctuations due to different samples are possible, but the differences are significantly smaller than the effects found by comparison of the powder and the composites.

At the first glance, the values observed for the mass fractal dimensions d_f of the powders and silica in PDMS correspond to a diffusion limited ($d_f=1.7$) and reaction controlled ($d_f=2.1$) aggregation, respectively,⁴ whereas the $d_f=2.5$ of silica in SBR can be explained by a diffusion limited cluster-monomer aggregation within the model of Witten and Sander.¹⁶ It is worth mentioning that Schaefer *et al.*¹⁷ compared precipitated silica and precipitated silica dispersed in rubber, but found no differences concerning the mass fractal dimension of the aggregates. However, contrary to the mass fractal dimension listed in Table I, already for the pure silica $d_f=2.5$ is reported, which is even greater than the mass fractal dimension of the silica in PDMS. Due to the differences, it is unclear whether the clustering in silica powders may occur due to diffusion limited aggregation, e.g., due to H bonds between the next neighbors and reaction controlled aggregation. Therefore, this important question is addressed below in detail.

The scattering diagram of VN3 in the SBR matrix exhibits a pronounced second crossover and by the model function a radius of gyration of about 28 ± 1 nm is extracted. By fitting Eq. (2) using the range $0.008\text{ nm}^{-1} < q < 0.016\text{ nm}^{-1}$, a mass fractal dimension $d_f=1.52 \pm 0.03$ is obtained for the clusters. It is worth noting that although the fitting error of the radius is very small, the absolute value is influenced by d_f . If the whole q -range could be covered, then possibly a slightly different slope is obtained, due to the above mentioned deviations from the linearity.³⁷ The radius determined by applying the model function can be checked exploiting that the cluster size is inverse proportional to the position of the crossover q_c .²³ Using an interpolation function (logarithmic-normal distribution) around the maximum within a Kratky plot, as described by Ehrburger-Dolle *et al.*,⁴⁰ $q_c=0.04\text{ nm}^{-1}$ is obtained. The scattering diagram shown by Schaefer *et al.*¹⁷ exhibits a crossover corresponding to the aggregate size at $q_c=0.01\text{ nm}^{-1}$. Using a model function they obtained a radius of gyration of 93.2 nm. The ratios between the crossovers and the radii should be roughly the same and therefore an estimated radius of gyration of about $93.2\text{ nm}/4=23.3\text{ nm}$ is found. Keeping in mind the

two different fitting procedures used and the crude estimation of q_c by simply fitting an interpolation function the values agree very well.

Using Eq. (6) and $d_f=2.41$, a perimeter radius $R_{\text{cluster}}=39$ nm can be calculated. Exploiting the scaling relation $N=(R_{\text{cluster}}/R)^{d_f}$, the aggregation number of $N\approx 20$ is obtained. This is in the range of 10–100, which seem to be the typical number of particles in aggregates.¹⁷ It is worth mentioning that there are several procedures to achieve the aggregation number, even if there are several possibilities for calculating it from the scaling relation.^{21,43,44} However, the following discussion does not rely on differences in the absolute value due to the different ways and therefore possible consequences are not considered further. In the case of the pure silica (3), the radius of gyration seems to be greater. Due to the limited range an exact determination is difficult or even impossible. However, the model function can be used to make a rough estimate. If the scattering diagram of the pure silica (3) shows a crossover at the very low q -values, then a radius of gyration of about 50 nm is found. If, however, the crossover is slightly outside the observation window so that the radius of gyration already influences the scattering curve, but the crossover is not visible, then a radius of gyration of about 100 nm is estimated. These values correspond to perimeter radii of 82 and 164 nm, respectively, and are consistent with the observations of Schaefer *et al.*¹⁷ who covered a much broader range. By means of the scaling relation, thus a aggregation number is found, which varies between 28 and 89 particles within each aggregate. Although this is a crude approximation, the conclusion is possible that together with the increasing mass fractal dimension and shrinking aggregate size, the mean number of primary particles in the aggregates decreases. This leads to the important conclusion that the aggregate does not simply shrink due to a compaction, rather, a rupture of particles or a breakage of aggregates has to be included. However, since the estimation of the aggregation number of the pure silica is very crude, neither a breakage nor a rupture can be excluded.

The most important observations taken from Fig. 1 and Table I are that the aggregates of the silica in the composite are smaller and exhibit a higher mass fractal dimension than that of the pure silica. At larger length scales, these observations are attributed to external forces acting on both precipitated and pyrogenic silica.^{14–17} Such forces may be due to the mixing process of the composite, and can be divided in external ones resulting from the mixer itself and internal forces due to filler-filler and/or filler-polymer interactions during the mixing process. This could lead to a break up of clusters, a rupture of weak arms by decreasing the size simply by compacting the particles.⁷

In order to test whether these assumptions are suitable to explain the different morphologies, simply a pistil and a mortar are sufficient to study the influence of external forces acting on pure silica. By that means, the silica was milled a selected time and then a part was removed to perform the scattering experiments. This was continued several times in order to obtain the time dependency. As an example, Fig. 2 shows that the mass fractal dimension of the sample VN3 (1) grows with increasing grinding time. Figure 3 illustrates that

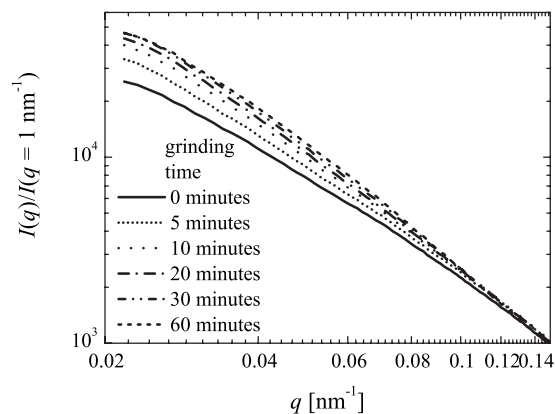


FIG. 2. Scattered intensity of pure silica as a function of q and various grinding times.

the same behavior is observed with the different precipitated silicas; additionally, the reproducibility is shown by the silica VN3 (1) and VN3 (2). The lines represent the mass fractal dimension of silica in the two different rubber composites. Furthermore Fig. 3 demonstrates that after 60 min, values are reached which are similar to the mass fractal dimension found in the silica-PDMS composite. This observation is further illustrated by Fig. 4, which compares the scattering diagrams of silica VN3 (1) milled for 60 min and silica in the PDMS matrix. Although it seems that the mass fractal dimensions tend to a constant value at long milling times, the mass fractal dimension of silica in SBR demonstrates that higher fractal dimensions are possible. Therefore, it is concluded that by increasing the forces and/or the grinding time, the mass fractal dimension will increase further. Of course, from the theoretical view, a maximum mass fractal dimension $d_f=3$ which reflects a compact and homogeneous three-dimensional object cannot be exceeded.

Although these results evidence that the mass fractal dimension of the silicas can be changed due to external mechanical forces, it still remains unclear whether the forces acting on the silica in the polymer matrix are due to the influence of the external mixer or because of the internal forces. This question can be further addressed by studying the composite and various silica fractions. By increasing the

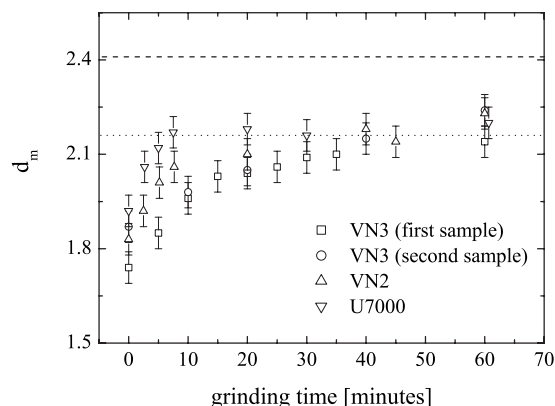


FIG. 3. Mass fractal dimension of pure silicas, VN3 (1), VN3 (2), VN2, and U7000, as a function of the grinding time. The dotted lines represent the value of d_f found for silica in PDMS ($d_f=2.16$) and silica in SBR ($d_f=2.41$).

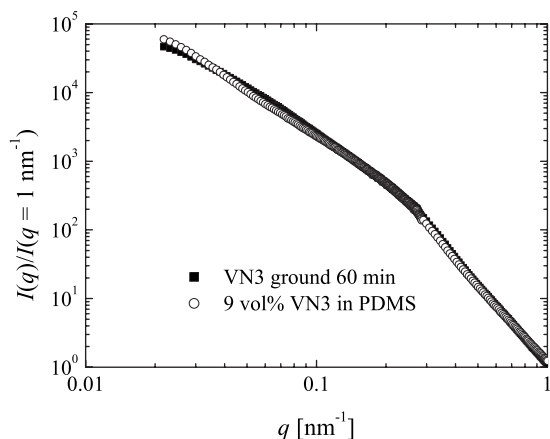


FIG. 4. Comparison of the scattered intensity as a function of q of pure silica ground 60 min and the silica-rubber nanocomposite.

silica fraction, the viscosity of the mixture enormously grows, which can be traced back to mutual interaction of the filler particles.^{9,14,15} As a simple model, one can assume that the distances between the particles are changed and therefore the shear forces involved. Furthermore, interactions of the polymer chains with the silica depend on the surface available.⁶ Both explanations provide a simple tool to explain why the shear forces acting on the clusters are higher if the filler fraction is enlarged. Figure 5 compares the scattering diagrams of the silica-PDMS composites for various silica fractions. Although the volume fraction of the filler varies from 9 up to 23 vol % almost no differences are observed. This is further illustrated by Fig. 6, which demonstrates that the mass fractal dimension does not depend systematically on the filler fraction. Therefore, the average value of $d_f=2.16$ can be calculated as illustrated by the line. Of course, since above the percolation threshold, collisions of silica particles are very likely, internal interactions somehow contribute to the change in the mass fractal dimension. However, the above results demonstrate that the internal interactions are of less importance if compared to the external influence. Therefore, it is concluded that the two different mass fractal dimensions of silica in the two composites are mainly due to differences in the mixing processes. However, a best possible proof of this conclusion would require a further

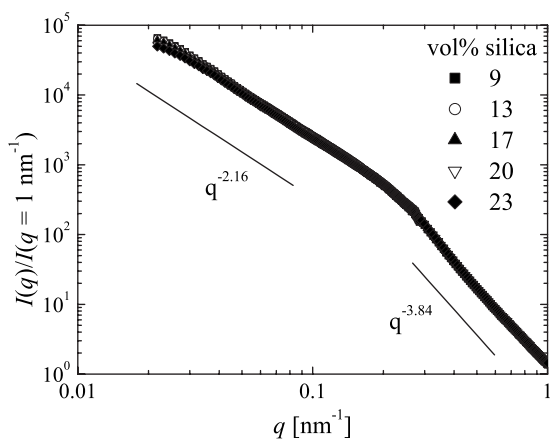


FIG. 5. Scattered intensity of silica in PDMS as a function of q and various volume fractions as indicated.

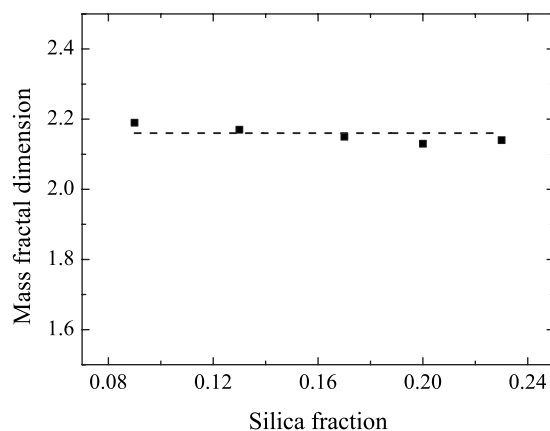


FIG. 6. Mass fractal dimension as a function of the silica fraction. The dotted line represents the average value $d_f=2.15$.

study. Finally, one should be aware that these conclusions refer only to the mixing process. No attempt is made to evaluate the influence of filler-filler interactions with respect to the mechanical properties of the composite material because evidences for such interactions are already reported in the literature.^{7,45,46}

The above experiments unambiguously demonstrate that due to the external forces during the mixing process, the mass fractal dimension of the aggregates increase. Furthermore a decrease in the size was observed. Therefore the morphology of pure silica and silica in the composites is different. Only very recently it was shown that the structure of aggregates of precipitated silica in PDMS can be changed simply by applying uniaxial external forces due to stretching of the rubber.¹³ Contrary, experiments on both precipitated and pyrogenic silica show that sonication does not affect the aggregate structure.¹⁴⁻¹⁷ At the first glance the experiments seem to be inconsistent. However, there are several differences concerning the samples which may explain the contradictions. On the first hand, the powder samples shown in the present work exhibit a mass fractal dimension of $d_f < 2$ and change to a maximum value $d_f \approx 2.5$. Contrary, e.g., Schaefer *et al.*¹⁷ report $d_f=2.5$ for the pure precipitated silica and no change by the external forces, neither by the sonication nor by the compounding. Possibly, if a pretreated silica is mixed in a polymer matrix, then no change would occur. However, as shown in the literature,¹³ it is very likely that even higher mass fractal dimensions than $d_f=2.5$ are obtained. On the other hand, it is possible that the solvent, necessary to perform the sonication process and the light scattering experiments, changes the mutual interactions. For example, due to the different environment of silica powder and silica in the solvent, possibly by the solvent molecules, interactions between the silica particles are mediated or created. This could probably lead to very strong bonds which result in very stable and strongly bonded aggregates, whereas the powder itself contains only weak aggregates. However, it should be mentioned that the experiments reported in the present work do not exclude strongly bonded primary particles. For example, it is possible that very small aggregates building a cluster cannot be distinguished unambiguously from a cluster formed by primary particles itself. Moreover, concerning the

light scattering results of the literature^{16,17} changes occurring in the mass fractal dimension of the aggregates probably are not resolved because of both the length scale involved and because of the multilevel structure of silica. Additionally, if pure silica is prepared for the microscopic experiments then a frequently applied technique is the dispersion of silica in a solvent such as, e.g., toluene. Then the solution is dropped onto the carrier and afterward dried. Only very recently was it observed that in this case, the particles reaggregate and larger structures are generated.⁴⁷ In such cases, the changes in the morphology reported by the present work are difficult to be observed by microscopic techniques. Due to the new findings in the present work, we conclude that in particular the preparation techniques seem to be of major importance. This does not only affect the microscopic techniques, e.g., transmission electron microscopy, where very thin composite samples are necessary, and therefore pure silicas dispersed in solvent or silica washed out from the polymer matrices are preferentially studied.⁹ It is, in particular, of importance if scattering experiments on the pure silica dispersed in a solvent are applied because the structure observed by means of such techniques is probably different from the true morphology present in the composite or in the powder. Moreover, comparing the structure of the pure silica with the mechanical properties of the composite may be questionable because as shown above, it is likely that the morphology is different. However, due to the results provided above it is very likely that it is possible to pretreat the silica particles by mechanical forces and then to obtain a better mixture.

Usually, silica is characterized by a few constitutive parameters, such as, e.g., the Brunauer, Emmett, and Teller (BET) surface area, which is a widely used technique for estimating the surface area by gas adsorption. In the case of the silicas studied above, the BET surface area is 170 m²/g (VN3/U7000) and 125 m²/g (VN2).⁹ Obviously the results does not or at least does not significantly depend on this number. The same result is obtained for the other parameters such as the cetyltrimethylammonium bromide surface area or the n-dibutyl phthalate absorption number. Perhaps the differences in these values are too small to be reflected by the above experiments.

Finally, possible reasons addressing the increase in the mass fractal dimension should be discussed. The experiments demonstrate that the aggregates are smaller and contain lesser primary particles within the SBR composite if compared to the pure silica. Therefore, it is very tempting to assume further correlations between d_f , N , and R_{cluster} beyond the scaling relation applied above. However, a decrease in the aggregate size is not necessarily connected to an increase in the mass fractal dimension.²¹ This is exemplified by a simple homogeneous object which has a mass fractal dimension $d_f=3$. If such a sample is broken in two pieces, then the mass fractal dimension of both subunits is still $d_f=3$. Therefore, a simple break up of the aggregates would not necessarily explain the change in the mass fractal dimension. However, as shown by the literature, silica aggregates possess only a few weak arms if any but more or less loosely packed primary particles.^{13,21,42} Therefore, a simple compac-

tion by a reduction in the distances of the primary particles including possible weak arms supported by a breakup of clusters is most likely.

V. CONCLUSIONS

Pure silicas as well as silica filled composites were studied by means of SAXS experiments. It was evidenced that the mass fractal dimension as well as the aggregate size is different if the pure silica and silica in composites are compared. The differences can be mainly attributed to the mechanical forces acting during the mixing process. This was proven by applying a pestle and mortar to the pure silica. Therewith, a systematic increase in the mass fractal dimension with growing grinding time was found. As an important drawback of both results, it would be questionable whether it is sufficient to correlate the morphology of pure filler and the viscosity of the silica-rubber mixture. Additionally the experiment demonstrates that a decrease in the cluster size is possible even before the silica is dispersed in rubber. Probably, this would decrease the mixing time and thus reduce chain degradation and therefore could result in improved materials. However, more importantly, the comparison of different pure silica samples demonstrates that without knowing their history the interpretation of the results may be difficult or questionable. Furthermore, it becomes evident that is not sufficient to provide only a description of the materials, rather, the details of the sample treatment have to be known.

ACKNOWLEDGMENTS

Many thanks to the beamline staff, Sabine Cunis, Stephan V. Roth, and Rainer Gehrke (BW4 HASYLAB/DESY, Germany), for help and technical assistance. The financial support of the experiments by the HASYLAB/DESY is gratefully acknowledged.

- ¹A. Einstein, *Ann. Phys.* **19**, 289 (1906).
- ²A. Einstein, *Ann. Phys.* **34**, 591 (1911).
- ³W. Niedermeier, H. Raab, J. Stierstorfer, S. Kreitmeier, and D. Göritz, *Kautsch. Gummi Kunstst.* **47**, 799 (1994).
- ⁴T. A. Witten, M. Rubinstein, and R. H. Colby, *J. Phys. II* **3**, 367 (1993).
- ⁵D. J. Kohls and G. Beaucage, *Curr. Opin. Solid State Mater. Sci.* **6**, 183 (2002).
- ⁶T. A. Vilgis, *Polymer* **46**, 4223 (2005).
- ⁷M. Klüppel, *Adv. Polym. Sci.* **164**, 1 (2003).
- ⁸J. N. Mrgudich and R. C. Clock, *Trans. Electrochem. Soc.* **86**, 351 (1944).
- ⁹H. D. Luginsland, *A Review on the Chemistry and the Reinforcement of the Silica-Silane Filler System for Rubber Applications* (Shaker Verlag, Aachen, 2002).
- ¹⁰S. K. Friedlander, H. D. Jang, and K. H. Ryu, *Appl. Phys. Lett.* **72**, 173 (1998).
- ¹¹F. Ehrburger-Dolle, F. Bley, E. Geissler, F. Livet, I. Morfin, and C. Rochas, *Macromol. Symp.* **200**, 157 (2003).
- ¹²A. Botti, W. Pyckhout-Hintzen, D. Richter, V. Urban, E. Straube, and J. Kohlbrecher, *Polymer* **44**, 7505 (2003).
- ¹³G. J. Schneider, *J. Chem. Phys.* **130**, 234912 (2009).
- ¹⁴B. B. Boonstra, H. Cochrane, and E. M. Dannenberg, *Rubber Chem. Technol.* **48**, 558 (1975).
- ¹⁵B. B. Boonstra, E. M. Dannenberg, and F. A. Heckman, *Rubber Chem. Technol.* **47**, 1082 (1975).
- ¹⁶D. J. Kohls, Ph.D. thesis, University of Cincinnati, Cincinnati, OH, 2006.
- ¹⁷D. W. Schaefer, C. Suryawanshi, P. Pakdel, J. Ilavsky, and P. R. Jemian, *Physica A* **314**, 686 (2002).
- ¹⁸R. Gehrke, *Rev. Sci. Instrum.* **63**, 455 (1992).

- ¹⁹ R. Gehrke, M. Bark, D. Lewin, and S. Cunis, *Rev. Sci. Instrum.* **66**, 1354 (1995).
- ²⁰ S. V. Roth, R. Döhrmann, M. Dommach, M. Kuhlmann, I. Kröger, R. Gehrke, H. Walter, C. Schroer, B. Lengeler, and P. Müller-Buschbaum, *Rev. Sci. Instrum.* **77**, 085106 (2006).
- ²¹ A. Bunde and S. Havlin, *Fractals and Disordered Systems*, 2 (Springer-Verlag, Berlin, 1995).
- ²² G. Beaucage, D. W. Schaefer, T. Ulibarri, and E. Black, *Polym. Mater. Sci. Eng.* **70**, 268 (1993).
- ²³ A. Hasmy, R. Vacher, and R. Jullien, *Phys. Rev. B* **50**, 1305 (1994).
- ²⁴ R. Hosemann and S. N. Bagchi, *Direct Analysis of Diffraction by Matter* (North-Holland, Amsterdam, 1962).
- ²⁵ G. Beaucage and D. W. Schaefer, *J. Non-Cryst. Solids* **172**, 797 (1994).
- ²⁶ G. Beaucage, *J. Appl. Crystallogr.* **28**, 717 (1995).
- ²⁷ G. Beaucage, *J. Appl. Crystallogr.* **29**, 134 (1996).
- ²⁸ G. Beaucage, J. H. Aubert, R. R. Lagasse, D. W. Schaefer, T. P. Rieker, P. Erlich, R. S. Stein, S. Kulkarni, and P. D. Whaley, *J. Polym. Sci., Part B: Polym. Phys.* **34**, 3063 (1996).
- ²⁹ D. W. Schaefer, T. Rieker, M. Agamalian, J. S. Lin, D. Fischer, S. Sukumar, C. Chen, G. Beaucage, C. Herd, and J. Ivie, *J. Appl. Crystallogr.* **33**, 587 (2000).
- ³⁰ J. Teixeira, in *On Growth and Form, Fractal and Non-Fractal Patterns in Physics*, edited by H. E. Stanley and N. Ostrowsky (Martinus Nijhoff, Boston, 1986), p. 145.
- ³¹ J. Teixeira, *J. Appl. Crystallogr.* **21**, 781 (1988).
- ³² C. Oh and C. M. Sorensen, *J. Colloid Interface Sci.* **193**, 17 (1997).
- ³³ M. Kotlarchyk and S.-H. Chen, *J. Chem. Phys.* **79**, 2461 (1983).
- ³⁴ J. Pedersen, *J. Appl. Crystallogr.* **27**, 595 (1994).
- ³⁵ J. Pedersen, *Adv. Colloid Interface Sci.* **70**, 171 (1997).
- ³⁶ M. Kölbl, Master's thesis, Universität Regensburg, 1998.
- ³⁷ R. Jullien, *J. Phys. (France)* **2**, 759 (1992).
- ³⁸ D. W. M. Marr, M. Wartenberg, K. B. Schwartz, M. M. Agamalian, and G. D. Wignall, *Macromolecules* **30**, 2120 (1997).
- ³⁹ T. P. Rieker, M. Hindermann-Bischoff, and F. Ehrburger-Dolle, *Langmuir* **16**, 5588 (2000).
- ⁴⁰ F. Ehrburger-Dolle, M. Hindermann-Bischoff, F. Livet, F. Bley, C. Rochas, and E. Geissler, *Langmuir* **17**, 329 (2001).
- ⁴¹ R. J. Young, D. H. A. Al-Khudhairy, and A. G. Thomas, *J. Mater. Sci.* **21**, 1211 (1986).
- ⁴² G. J. Schneider, S. A. Fink, R. Rachel, and D. Göritz, *Kautsch. Gummi Kunstst.* **9**, 461 (2005).
- ⁴³ G. Beaucage, H. K. Kammler, and S. E. Pratsinis, *J. Appl. Crystallogr.* **37**, 523 (2004).
- ⁴⁴ H. Peterlik and P. Fratzl, *Monatsch. Chem.* **137**, 529 (2006).
- ⁴⁵ A. R. Payne, *J. Appl. Polym. Sci.* **6**, 57 (1962).
- ⁴⁶ A. R. Payne, *J. Appl. Polym. Sci.* **7**, 873 (1963).
- ⁴⁷ D. Sen, S. Mazumder, J. S. Melo, A. Khan, S. Bhattacharya, and S. F. D'Souza, *Langmuir* **25**, 6690 (2009).